JOURNAL OF PROPULSION AND POWER
Vol. 13, No. 5, September–October 1997

Jet Engine Component Maps for Performance Modeling and Diagnosis

G. Sieros,* A. Stamatis,† and K. Mathioudakis‡
National Technical University of Athens, Athens 157 10, Greece

This paper describes an effort to model the performance maps of compressors and turbines (i.e., the relation between mass flow, pressure ratio, and efficiency), using analytical functions. Analytical functions are fitted to the available experimental data using a least-squares-type approach for determining the parameters of the fitting function. The success of using a particular function for an application is assessed through a suitably defined mean error of the model. Apart from presenting the method for setting up these analytical representations, applications to performance modeling and fault diagnosis are discussed. The change in model parameters is used to characterize changes of the engine condition and possibly diagnose occurring faults. The impact of introducing analytical component models into overall engine computer models, replacing a tabulated form of the component maps, is also discussed.

Nomenclature

F_f = flow function, Eq. (18)
h_t = total enthalpy
$\dot{m}$ = mass flow
N = rotational speed, rpm
$\bar{n}$ = nondimensional rotational speed
P_f = power function, Eq. (18)
P_t = total pressure
T_t = total temperature
X, Y = transformed values of the map variables
x, y = raw values of the map variables
α_i = parameters of the analytical functions
Δh_t = enthalpy drop in the turbine
δ = $P_t/P_{t\text{-REF}}$
η_c = compressor adiabatic efficiency, total–total
η_T = turbine adiabatic efficiency, total–total
θ = $T_t/T_{t\text{-REF}}$
ι = corrected mass flow, $\dot{m}\cdot\sqrt{\theta}/\delta$
Π = compressor pressure ratio

Subscripts
REF = value at a reference point
sl = value at the surge line

I. Introduction

THE performance maps of the turbomachinery components of a jet engine, namely, compressors and turbines, constitute an essential input to overall engine performance models. The maps are usually introduced in the form of tabulated functions, and interpolation is used for obtaining the values of dependent parameters corresponding to arbitrary values of the independent ones. Simplifying the map representation, by using analytical functions, is highly desirable because it adds flexibility to an engine model, while it can give additional possibilities for component condition assessment.

The present work has been stimulated mainly by the possibilities it offers for application in the field of engine condition monitoring and fault diagnosis. Analytical representations provide the possibility of direct estimation of component performance alterations, when either steady-state or transient performance data are available. This kind of application has been discussed by Bird and Schwartz.[1] Another advantage is the possibility of reducing the running time of a model on a digital computer, a desirable feature, especially in engine control applications.[2] A useful feature for both types of applications is the smooth character of analytical representations in comparison to tabulated functional ones.

In the present paper, a method of constituting analytical representations for both compressor and turbine maps is presented. The aim is to produce functions that contain as few parameters as possible, and to reproduce as reliably as possible a performance map obtained either by experiment or computation. Methods of this type have already been employed by previous authors,[3,4] always as a part of an engine performance model. In these papers[3,4] some particular analytic relations have been employed, without particular attention to how well such relations represent actual compressor maps. This question was first tackled systematically by El-Gammal[2]; he employed what we term linear models for map representation, and established a set of criteria for assessing the success of the approximation for a map given as a set of data points.

The method introduced in the present paper constitutes a further advancement of analytic modeling methodology. The main innovation is the possibility of using different functional forms of representation, which give the possibility to successfully model maps of different types of designs. Extensive validations are presented by application to actual data from components of several gas turbine engines. The method is formulated in such a way that the choice of the appropriate function among a large number of function classes can be effected in a systematic way, when a new application is attempted.

II. Method of Formulation of Analytical Relations

The customary way of presenting performance maps of a compressor or a turbine is by means of a set of curves, which express the relation of mass flow rate (or a corresponding flow function) to pressure ratio and efficiency for different values of a speed parameter. A typical form of a compressor map appears in Fig. 1.

The purpose of the present method is to derive explicit analytical expressions for the relations represented by these curves. The starting point are the sets of performance parameters values that constitute the curves of a map. The steps necessary to obtain the analytical expressions are described next.

Received Oct. 21, 1995; revision received April 16, 1997; accepted for publication May 9, 1997.

*Postgraduate Student, Laboratory of Thermal Turbomachines, Department of Mechanical Engineering, Fluids Section.
†Research Engineer, Laboratory of Thermal Turbomachines.
‡Assistant Professor, Laboratory of Thermal Turbomachines.

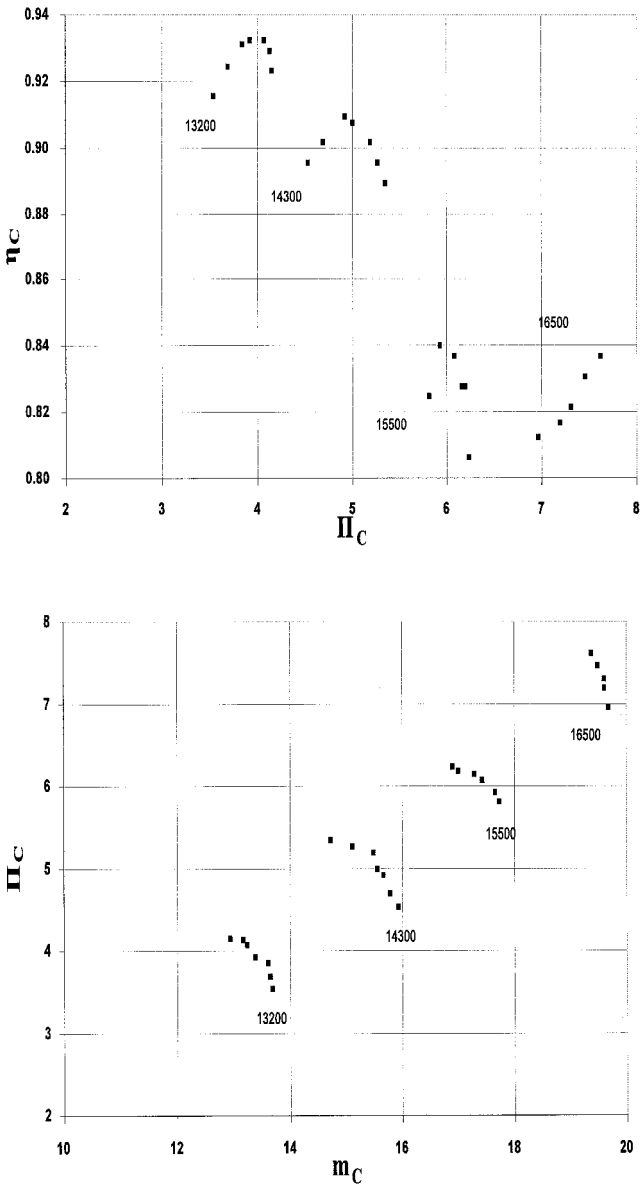

Fig. 1 Compressor performance map (J85 engine compressor[8]).

A. Data Scaling

The actual values of the various quantities may be of different numerical magnitude. Additionally, the various quantities may vary significantly with the engine's rotational speed. This may introduce an inaccuracy in the derivation of an explicit relation between these quantities and the engine's speed, because the different magnitude of the various quantities implies that they are not discretized with the same accuracy. For this reason, the data are scaled with reference to appropriate values. The surge line provides such values for the compressor. For the turbine, a point along the choking part of a characteristic can be chosen. In correspondence to compressors, the point on the limit load line are a suitable choice, covering maps corresponding to both low- and high-reaction designs.

The surge line itself is represented as a second- or third-degree polynomial function of rotational speed, so that the mass flow, pressure ratio, and efficiency at the surge line can be expressed in the following form:

$$\dot{m}_{Csl} = \dot{m}_{Csl}(N) \qquad \Pi_{Csl} = \Pi_{Csl}(N) \qquad \eta_{Csl} = \eta_{Csl}(N)$$

Having expressed the surge line in such a way, we can scale the respective quantities as $\dot{m}_C = \dot{m}_C/\dot{m}_{Csl}$, $\Pi_C = \Pi_C/\Pi_{Csl}$, $\eta = \eta/\eta_{sl}$. The rotational speed is also scaled with respect to its maximum value, giving the corrected speed $\bar{n} = N/N_{REF}$.

Figure 2 depicts the representation of a typical compressor surge line (in this case it is the mass flow that is represented, but the same applies to pressure ratio and efficiency) with the use of a polynomial function; Fig. 3 shows the scaled map.

B. Transformation of Variables

The scaled variables of a map are transformed to formulate quantities whose relation to each other can be described with the use of simpler (e.g., linear) analytical functions.

A pair of parameters (x, y) is thus transformed to a new pair (X, Y). For example, we may have $x = \dot{m}\sqrt{\theta}/\delta$ and $y = \Pi_c$, which transform to $X = x$, $Y = y/x$. The actual transformations used will be described in the following section. Figure 4 illustrates the transformed variables for the map of Fig. 3, using a transformation that makes their relation linear.

C. Model Formation

Having completed the previous steps, we dispose of a set of variables that need to be interrelated, using an analytical expression. The requirement is that the map, available in the form of tabulated data points, should be represented with the greatest possible accuracy. To do that we will use an analytical expression with the general form

$$Y = F(X, \bar{n};\ a), \qquad a = (\alpha_1, \alpha_2, \ldots, \alpha_N) \tag{1}$$

where $\bar{n}$ is the corrected speed, and a is the array of the model

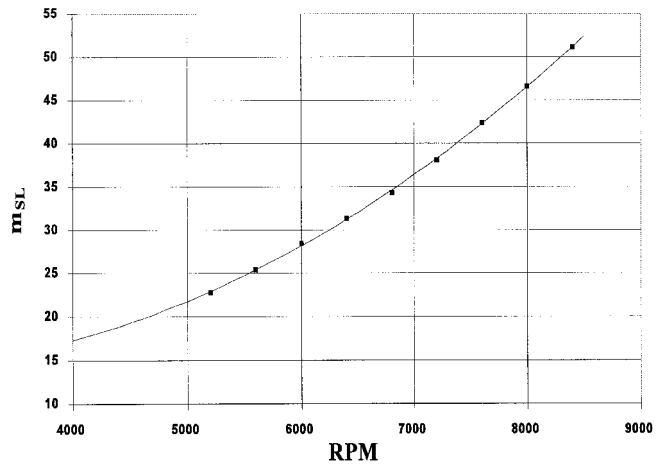

Fig. 2 Mass flow as a function of rpm for the ATAR engine surge line.

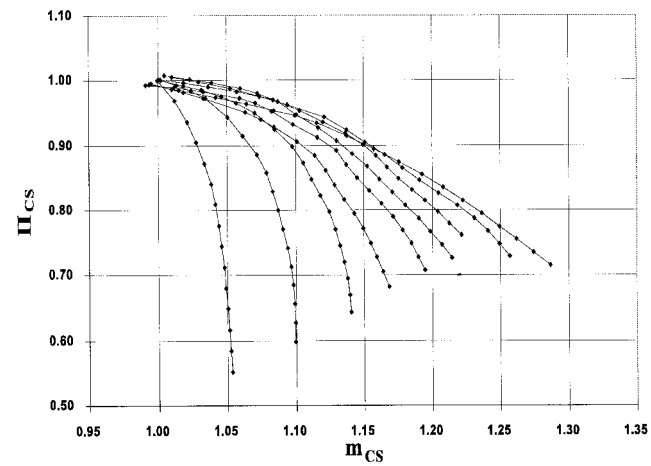

Fig. 3 Scaled map for the ATAR compressor.[7]

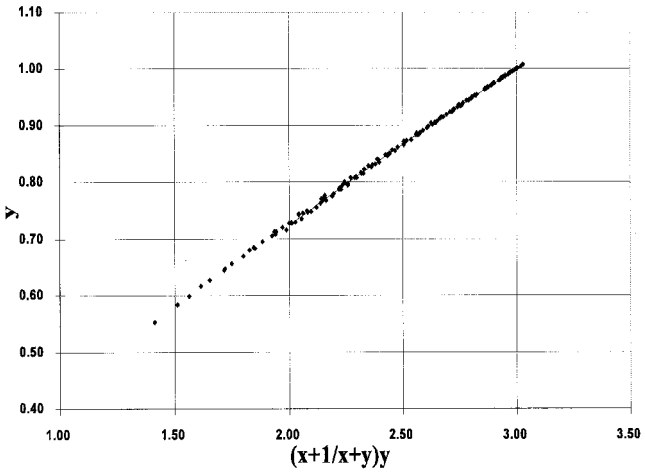

Fig. 4 Transformed mass flow-pressure ratio map for the ATAR compressor.

parameters. The values of these parameters will be determined using a least-squares method.

This expression for the desired function can be cumbersome, and the infinity of existing functions F makes it difficult to find one that is satisfactory. For this reason, we limit our search to certain classes of functions. In the present work, two categories of models were examined. The first is the generalized linear model, using a function of the form

$$Y = \sum_{i=1}^{N} \alpha_i \cdot F_i(X, \bar{n}) \tag{2}$$

This type of model is termed linear, because it is linear with respect to the parameters α_i, but not necessarily for the variables X, Y.

Further simplifying the previous expression, we may separate the influence of $\bar{n}$ and X, by

$$Y = \sum_{i=1}^{K} \left\{ \left[\sum_{j=1}^{M} \alpha_{ij} s_{ij}(\bar{n}) \right] f_i(X) \right\} \tag{3}$$

This is the form that will be used for generalized linear models.

The second category consists of nonlinear models, in the form

$$Y = F[X;\ a(\bar{n})] \tag{4}$$

where the influence of $\bar{n}$ is again separated from that of X.

In the section that follows, specific types of functions will be presented. These functions are chosen by referring to the usual form of compressor and turbine maps, reflecting the physics of their operation.

D. Parameter Calculation

The parameter array a for linear and nonlinear models is calculated using a least-squares method. The methodology used for linear and nonlinear models is described in the Appendix.

E. Error Estimation

The final step is to estimate the error in the description of the engine map for a given model. This is an essential step because it gives an assessment of the success of the approximation.

The following formula was used to estimate the mean error:

$$\overline{\text{err}} = \sum_{i=1}^{\text{NP}} \left| \frac{y_i - \hat{y}(x_i)}{y_i} \right| \Big/ \text{NP} \tag{5}$$

For a certain map, x_i, y_i is the measured value and y is the calculated value by the model. This formula can be used either for the entire map or for parts of it; e.g., a speedline.

In addition to the model error, which is critical for simulation purposes, it is also desirable to determine the probable error in the parameter calculation. This second error is important in diagnostic applications, where it is necessary to distinguish between statistically significant and random changes of parameters, to make a decision about the presence of a fault. For parameter α_j, a relation of the following form is established:

$$\alpha_j = \alpha_{j(\text{calc})} \pm (\text{probable error})$$

The procedure for determining not only the value, but also the confidence region for a parameter, is described in the Appendix.

To clarify the implementation of the method described previously, specific types of applications are described in the following sections. First, the use of the model for the reproduction of compressor and turbine maps of aeroengines and industrial gas turbines will be demonstrated. A comparison to experimental data shows that an accurate representation of these maps is possible in all cases. Next, use of the present method for diagnostic applications will be demonstrated. Finally, analytical component models are incorporated in a complete engine performance model, and the impact it has in comparison to tabulated representations is discussed.

III. Analytical Representations of Compressor and Turbine Maps

Particular forms of functions representing compressor and turbine maps are now presented. The purpose of this presentation is to demonstrate the degree of accuracy obtained with different types of functions, while providing the main forms of functions the authors have found suitable for each case. Prior to presenting the particular functions, it is useful to discuss the physical reasoning behind the choice of a particular type of function.

A. Compressor Maps

The nature of the flow in compressors leads to a form of maps that is distinctly different and more complicated than those of turbines.[5] Even though one can start from a simple representation in terms of nondimensional parameters (the flow and load coefficients), the $m - \pi_c$ characteristics of a compressor are expressed as transcendental expressions in terms of the simple variables.[6] To represent a speedline, it is thus essential to use nonlinear expressions. On the other hand, especially at high speeds, parts or all of a speedline may be almost perpendicular to the mass flow axis, since chocking at some blade rows freezes the mass flow parameter. Another feature of a high-speed compressor map is that the speedlines come closer together as the speed increases.

To represent the nonlinearity, expressions that are at least second degree between the reduced variables are employed. The existence of vertical parts is represented by terms that are ratio of quantities, thus giving the possibility for representing asymptotes at the zeros of the denominator. An alternative is the use of continuous, smooth piecewise expressions. The inclusion of logarithmic or exponential functions gives the possibility for better representations of transcendental functions. Finally, the change in distance between speedlines with the same speed increment is taken into account by using the nonlinear expression for the surge line used as reference for nondimensionalization, as mentioned earlier. To assess how accurate the representation by the different functions is, we used the maps of numerous compressors, including those of the ATAR (Ref. 7) and J85 (Ref. 8) aeroengines, and that of the Typhoon[9] industrial gas turbine. These maps came in the $\dot{m}$, Π_c, and η_c forms, respectively.

To represent the $\dot{m}-\Pi_c$ map, we denote $x = \dot{m}$, $y = \Pi_c$; whereas for the $\Pi_c-\eta_c$ map, we choose $x = \Pi_c$ and $y = \eta_c$. We scale the variables with respect to the surge line that is represented by second- or third-degree polynomials.

1. Simple Linear Models

In this case, it is our purpose to transform the variables in such a way that $Y = \alpha_1 + \alpha_2 X$, so that only two parameters need to be determined. A pair of transformations used was

$$Y = x + y, \qquad X = \bar{n}\cdot(x - y)^2 \quad (\dot{m}-\Pi_c \text{ map}) \tag{6}$$

for which the mean error was between 2.50–3.20% for the examined compressors. A similar method for the $\Pi_c-\eta_c$ map was

$$Y = (x + y)^2, \qquad X = (x + y + 1/x)\cdot(x + y) \quad (\Pi_c-\eta_c \text{ map}) \tag{7}$$

with a mean error between 0.75–1.20%.

Even though such simple two-parameter models do not provide a high degree of accuracy for map representation, their usefulness lies in the possibility they offer for diagnostic purposes, as will be discussed in this paper.

2. Generalized Linear Models

We will start again from the representation of the $\dot{m}-\Pi_c$ map. The simplest form of such models is

$$Y = \alpha_1(\bar{n}) + \alpha_2(\bar{n})\cdot X \tag{8}$$

where α_1 and α_2 are expressed as polynomials. One of the transformations that gave good results was Eq. (6), with first-degree polynomials:

$$\alpha_1 = \alpha_{11} + \alpha_{12}n, \qquad \alpha_2 = \alpha_{21} + \alpha_{22}n$$

The mean error for this case was between 1.00–2.00%, and can be further reduced to <1.5% if we use a second-degree polynomial for α_2, raising the total number of parameters to 5.

A further increase in accuracy is achieved by using a second-degree polynomial in the form

$$Y = \alpha_1(\bar{n}) + \alpha_2(\bar{n})\cdot X + \alpha_3(\bar{n})\cdot X^2 \tag{9}$$

where $\alpha_i(n)$ are again polynomials. The best results with this form of function were obtained for the transformation

$$X = (x + y)^2\cdot\bar{n}, \qquad Y = y \quad \text{or} \quad Y = \sqrt{y} \tag{10}$$

for which the mean error was <1% for most of the test compressors.

The parameters for this model were given in the form of polynomials of varying degrees

$$\alpha_1 = \alpha_{11}, \quad \alpha_2 = \alpha_{21} + \alpha_{22}\cdot\bar{n} + \alpha_{23}\bar{n}^2, \quad \alpha_3 = \alpha_{31} + \alpha_{32}\cdot\bar{n} \tag{11}$$

giving a total of six parameters. The results of this model appear in Fig. 5 (reproduced map vs original map) and Fig. 6 (mean error in the estimation of $\dot{m}$ for a given pressure ratio).

In the error estimation, we include not only the overall mean error, but also the mean error for every characteristic of the map. It is seen from this representation that not all the curves are represented with the same accuracy. In this case, for example, even though the overall reproduction of the map is quite good, there are certain areas where the error is substantially higher than the mean error.

A similar model used with encouraging results was

$$Y = \alpha_1(\bar{n}) + \alpha_2(\bar{n})\cdot X + \alpha_3(\bar{n})\cdot e^X, \quad \text{with} \quad X = x/y, \quad Y = y \tag{12}$$

The mean error did not change considerably for the examined compressors, but the formula is included as it might prove superior in other cases. A representation of the map by a model of this kind appears in Fig. 7.

Switching to the representation of the $\Pi_c-\eta_c$ map, and starting with the simpler models of the form described by Eq. (8),

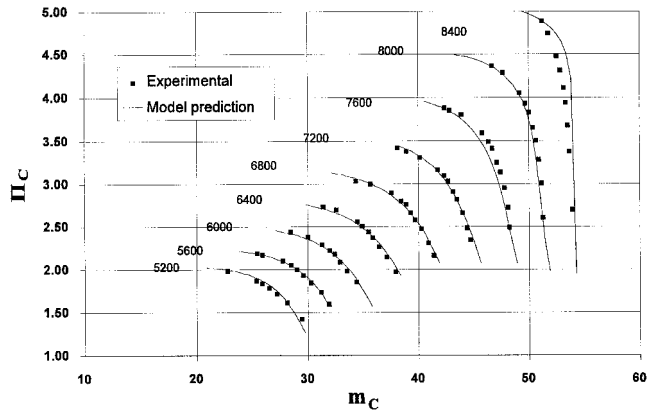

Fig. 5 Mass flow–pressure ratio map for the ATAR engine compressor.

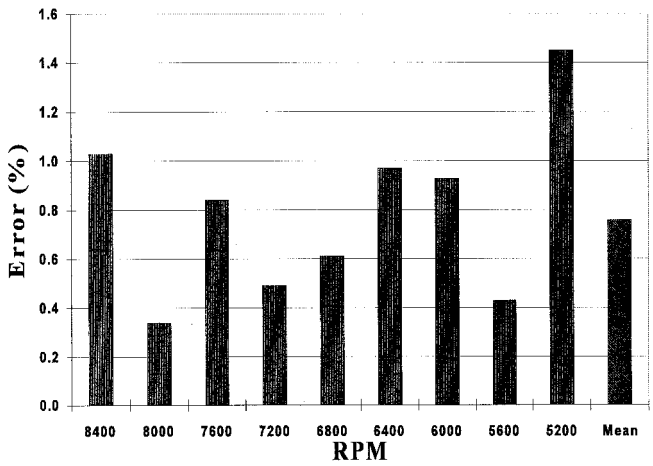

Fig. 6 Mean error for the ATAR compressor map representation.

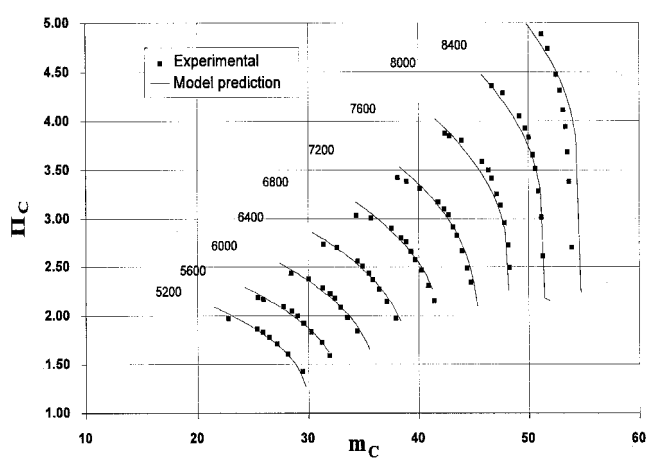

Fig. 7 Mass flow–pressure ratio map for the ATAR (Ref. 8) compressor.

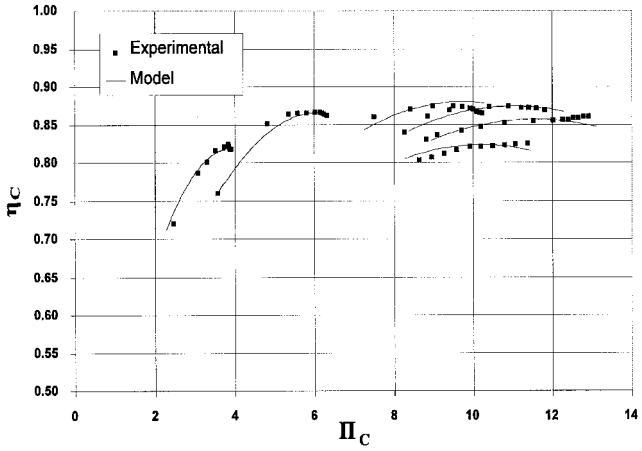

Fig. 8 Pressure ratio–efficiency map for a typical compressor.

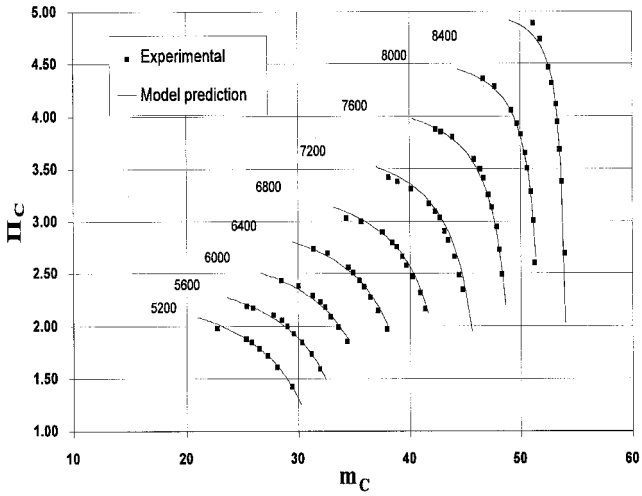

Fig. 9 Reproduction of the mass flow–pressure ratio map for the ATAR (Ref. 8) compressor.

the use of the following transformations resulted in a mean error <0.90% for the examined compressors:

$$X = \frac{x}{(y \cdot \bar{n})}, \qquad Y = y \tag{13}$$

Proceeding to more complicated models of the form described by Eq. (9), and using nontransformed variables ($X = x$, $Y = y$), we have a mean error of <0.50% for all of the test cases, and for modeling of the parameters α_i in the following form:

$$\alpha_1 = \alpha_{11} + \alpha_{12} \cdot \bar{n} + \alpha_{13} \cdot \bar{n}^2, \quad \alpha_2 = \alpha_{21} + \alpha_{22} \cdot \bar{n}, \quad \alpha_3 - \alpha_{31} \tag{14}$$

The use of nontransformed variables has the advantage that the $\eta_c = \eta_c(\Pi_c)$ relation is given in an explicit form. In addition to that, the minimization is performed on the actual values of x, y and not on a set of transformed variables X, Y, thus avoiding the introduction of an additional error. The use of this model is represented in Fig. 8.

We can use the same nontransformed variables in an expression of the following form:

$$Y = \alpha_1(\bar{n}) + \alpha_2(\bar{n}) \cdot X + \alpha_3(\bar{n}) \cdot \log(X) \tag{15}$$

and obtain results of the same accuracy using five instead of six parameters, modeling α_i as

$$\alpha_1 = \alpha_{11}, \quad \alpha_2 = \alpha_{21} + \alpha_{22} \cdot \bar{n}, \quad \alpha_3 = \alpha_{31} + \alpha_{32} \cdot \bar{n} \tag{16}$$

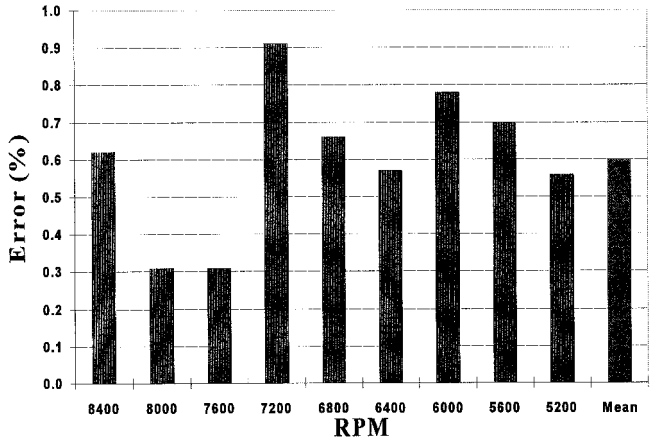

Fig. 10 Error in the reproduction of the compressor map for the ATAR engine.

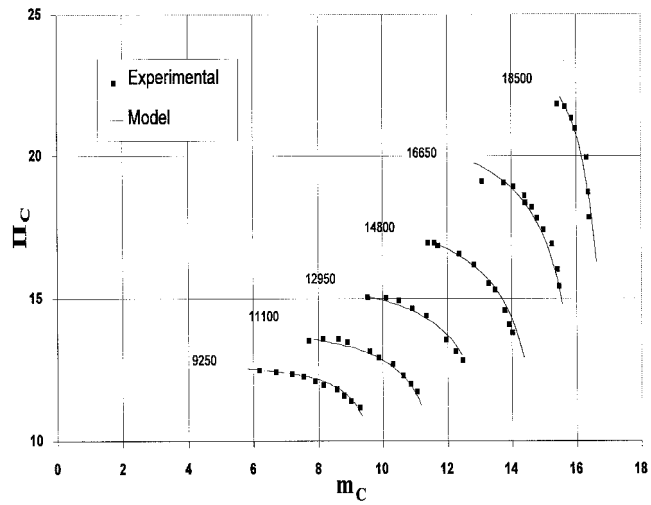

Fig. 11 Mass flow–pressure ratio map for the Typhoon (Ref. 9) compressor.

3. Nonlinear Models

These models offer the greatest versatility because they do not suffer from any restrictions (the chosen function can be of any form), and they can be applied without the need for parameter transformation. They were only used for the $\dot{m}-\Pi_c$ maps, since these maps presented the greatest difficulty.

The following expression resulted in mean errors of 1% for all of the examined compressors:

$$y = \alpha_1 + [\alpha_2/(x + \alpha_3)], \quad \alpha_1 = \alpha_{11} + \alpha_{12} \cdot \bar{n}$$
$$\alpha_2 = \alpha_{21} + \alpha_{22} \cdot \bar{n} + \alpha_{23} \cdot \bar{n}^2, \quad \alpha_3 = \alpha_{31} + \alpha_{32} \cdot \bar{n} \tag{17}$$

Additionally, the fact that this form has a vertical asymptote $x = -\alpha_3$, means that the high-speed ranges can be modeled in a way that is physically acceptable, as the tendency of the characteristics to become vertical at high speeds is predicted by the model. This model appears in Figs. 9 and 10 (for the ATAR compressor), and it reproduces the compressor map in a satisfactory manner. The same model, as applied to the Typhoon compressor, appears in Fig. 11; whereas the J85 compressor representation appears in Fig. 12.

B. Turbine Maps

The turbine maps available appeared in the P_f and F_f efficiency form, where

$$P_f = \dot{m} \cdot \Delta h_t / P_t \cdot \sqrt{T_t}, \qquad F_f = (\dot{m} \cdot \sqrt{T_t}/P_t) \cdot \bar{n} \tag{18}$$

The turbine maps have a form that can be considered simpler than that of compressors. It is even known that for multistage turbines a quadratic expression can be used to approximate the pressure ratio-mass flow characteristic.[10] Therefore, simpler polynomial expressions provide sufficient accuracy for modeling. For example, for $x = F_f$, $y = P_f$, the following expression, including four parameters, is adequate for a mean error <0.75% for all of the examined turbines:

$$y = \alpha_1 + \alpha_2 \cdot x + \alpha_3 \cdot x^2, \quad \alpha_1 = \alpha_{11} + \alpha_{21} \cdot \bar{n}$$
$$\alpha_2 = \alpha_{21}, \quad \alpha_3 = \alpha_{31} \tag{19}$$

If we use $X = x/y$, $Y = y$, and model $\alpha_1 \div \alpha_3$, using first-degree polynomials, the mean error drops to <0.40%.

A reproduced map, using the second model, appears in Fig. 13.

Using this transformation, we can even have constant $\alpha_1 \div \alpha_3$ (a total of three parameters), and still retain an error <0.75%, indicating that a transformation of this kind renders the variables practically independent of speed.

The $P_f - \eta_T$ map is also modeled with the function described by Eq. (19), but using first-degree polynomials for α_1 and α_2 and constant α_3. This modeling results in an error of <1% for the test cases, that can drop to <0.5% if we use a second-degree polynomial to model α_2. Figure 14 depicts the representation of the turbine map using this model.

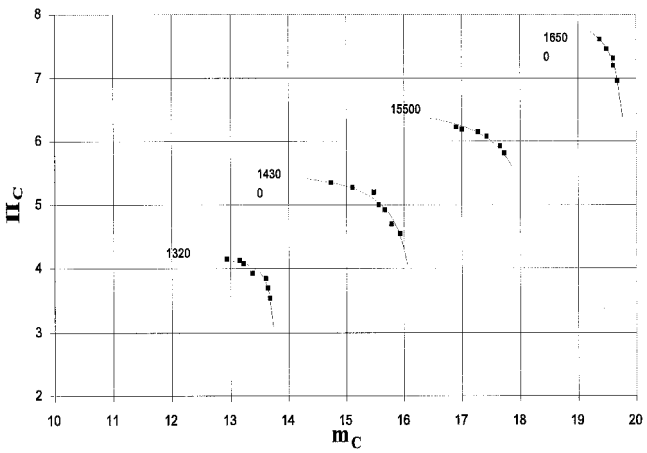

Fig. 12 Mass flow – pressure ratio map for the J85 (Ref. 8) engine compressor.

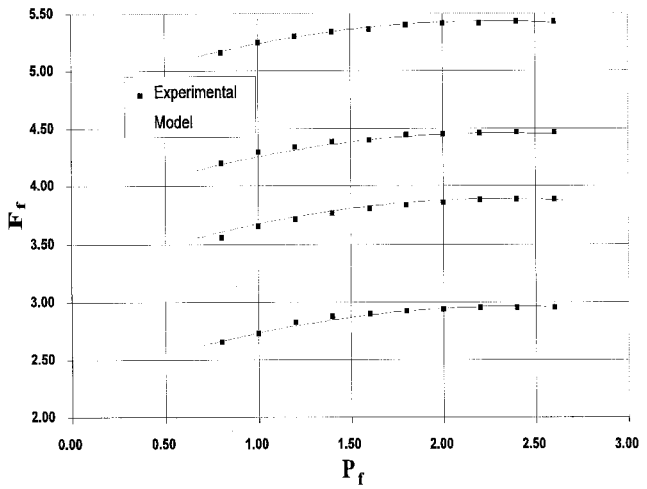

Fig. 13 Flow function – power function map for a typical turbine.

IV. Application to Performance Modeling and Diagnostics

Possibilities offered by utilizing an analytical representation of component maps within computer engine models are now examined.

A. Diagnostic Potential

When components maps are employed in an analytical form by an engine model, then the value of any measured quantity calculated by the model may be considered to be a function of the values of the component parameters. This interrelation can be expressed in the following form:

$$Y = F(\alpha_1, \alpha_2, \ldots, \alpha_n)$$

(α_i are the component model parameters). When measurements are available, this relation can be used to determine the values of α_i, and therefore, deduce component condition.

The diagnostic potential of the method will be displayed using an altered version of the experimental compressor and turbine maps, to examine the effect on the calculated parameters. For a compressor map we used the ATAR engine map and reduced the compressor's swallowing capacity by 2%. This situation would represent a deteriorated engine condition. Our purpose is to demonstrate how such a change in the map reflects on the parameters of an analytical expression. The initial and artificially transformed maps appear in Fig. 15.

Using a very simple two-parameter model (linear), we calculated the values of α_1, α_2 for the initial state and the modified one. In Fig. 16, we display the change in the value of these parameters. The change of each value is represented by a bar of

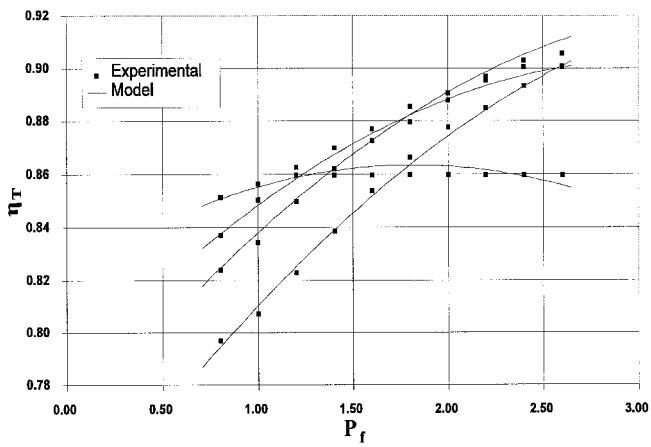

Fig. 14 Power function – efficiency map for a typical turbine.

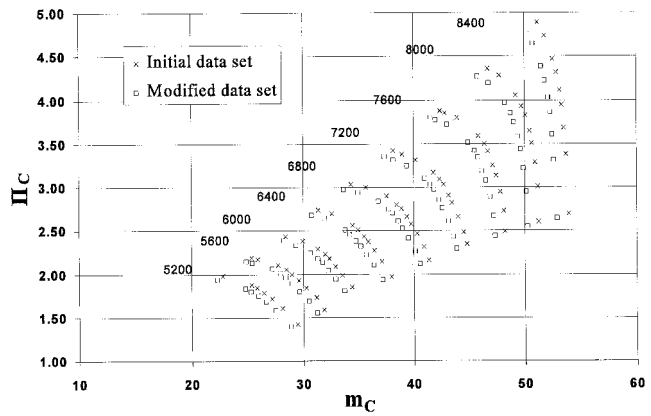

Fig. 15 Initial and modified map for the ATAR engine compressor.

a width equal to the statistical error in its estimation. It is obvious that the change of the map is reflected on the calculated parameters. What is more important is that this change is statistically significant.

A similar test was performed using a turbine map. In this case, we used a three-parameter model and introduced an error as described earlier. The initial and the modified maps are shown in Fig. 17.

In this case, the change was significant for only one of the three parameters. Different changes in the form of the map will result in different variations of some or all of the model parameters. The exact correlation between engine faults and parameter variations is a matter that needs to be further examined if diagnostic rules are to be derived.

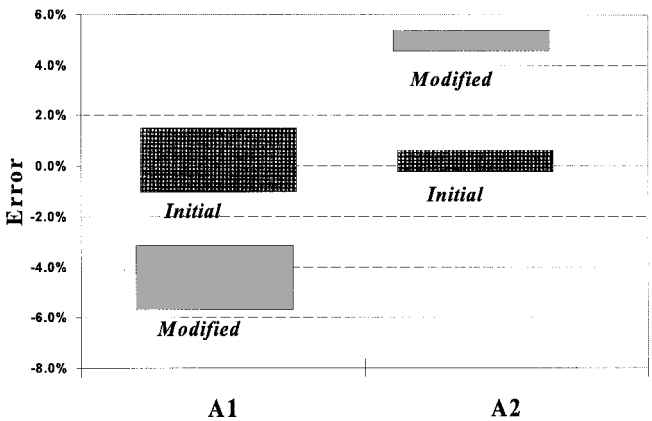

Fig. 16 Change of the parameters for an imposed change of the compressor map.

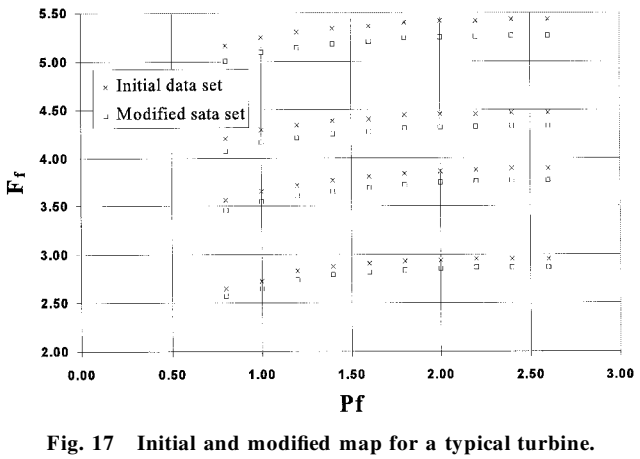

Fig. 17 Initial and modified map for a typical turbine.

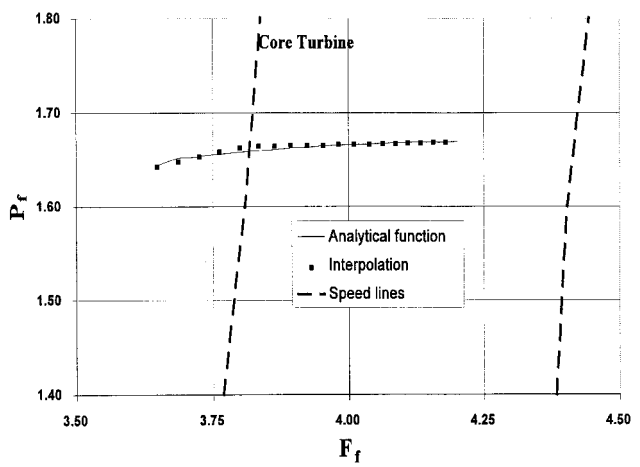

Fig. 18 Transitional behavior, as it appears on the turbine map (detail).

B. Engine Modeling

The models for compressor and turbine, that were described earlier in this paper, were subsequently introduced in a complete engine modeling program,[11] and they were used to predict the transient behavior of the engine in that program. A speed ramp is considered where the engine rpm increase with time. The representation of the working line (on the turbine map) that emerged from this modeling appears in Fig. 18, along with the respective line for the unmodified model that used interpolated values from the components' maps.

It is obvious that the analytical model results in smoother transition curves (a behavior closer to the actual one), while the steady-state condition does not differ; indicating that the function used is quite accurate in the prediction of the components' operating point.

V. Discussion of Application Aspects

In the applications presented earlier, different forms of functions have been considered. The question may arise as to how the appropriate functions are chosen. Methods that use software with a graphic user interface are now available to help even inexperienced users make this appropriate function choice. The software incorporates a number of possible variable transformations and element functions that allow the user to build a variety of possible analytic expressions of the linear or nonlinear type. The types of functions presented previously, for compressors and turbines, are expected to cover the majority of maps encountered in practice. When the model is fed with data from a map to be modeled, the user can build the form of function of this choice. Assessment of the approximation quality is provided by graphic display of the maps and the various error terms that characterize the accuracy of the approximation. It is thus easy to choose an optimum model for any application. A small sample of the options that this software offers appears in Fig. 19.

In diagnostic applications, the use of models that utilize a limited number of parameters may be advantageous, since the purpose of the model is not to reproduce the component map with the greatest accuracy. The effect of varying faults on the parameters of a model, especially when we use models with more parameters (e.g., Refs. 3, 8, 9, and 11), and the ability to distinguish between various kinds of engine malfunctions is an area that needs to be further examined.

The representation of component maps with analytical functions can also prove advantageous when complete models that simulate the engine's performance are used. In those cases, the use of such functions results in smoother, and therefore, physically more acceptable, curves that represent the transient operation of the engine. In addition, the use of analytical relations may result in faster calculations, compared to the use of a tabulated map with subsequent interpolations, when an explicit function is used. In a sample calculation of the transitional behavior of a twin-spool turboshaft that was performed, the use of analytical functions in the place of tabulated component maps resulted in a 40% reduction in computational time. This reduction does not represent a substantial gain in off-line computations, but it could prove very useful if the engine model is to be used for the real-time control of the engine.

It should be mentioned that the method proposed here covers, in the most general way, the problem of analytical representation. While previous authors[2–4] have considered particular forms of functions, the present method gives the possibility of a choice of function, a choice which is extended to functions of quite elaborate form. An additional possibility offered by the present method is the choice of a different function for the same map, according to the application envisaged. For example, for a particular engine, an elaborate expression

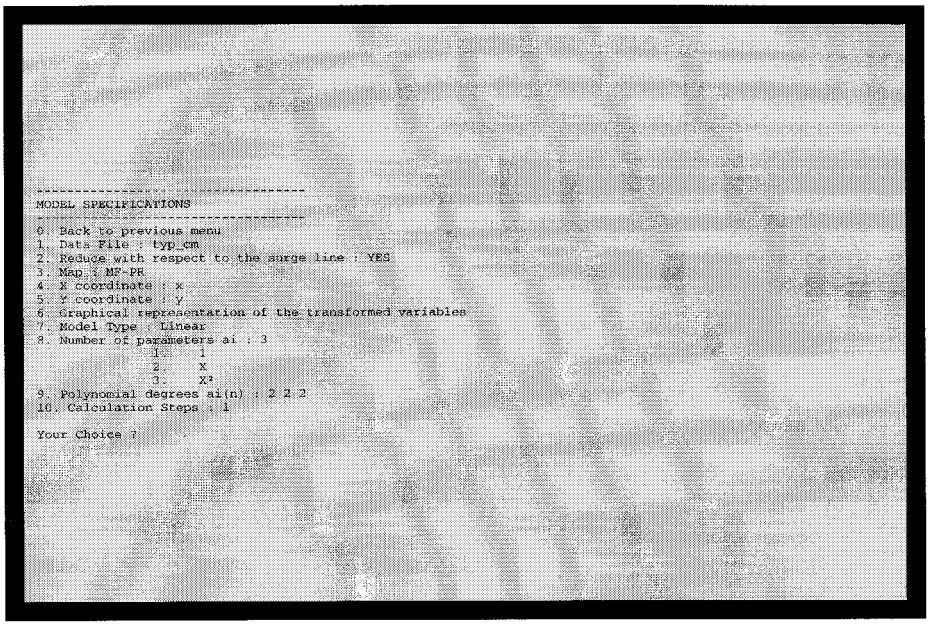

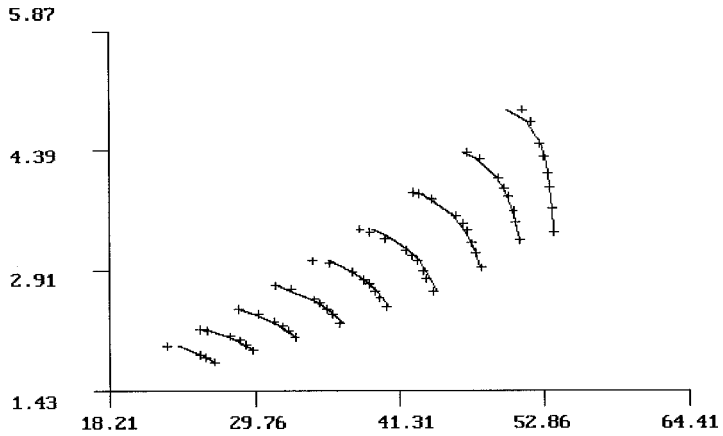

Fig. 19 Typical options screen along with a graphical representation of the specified model.

can be chosen for a map to be introduced in a transient model, while a much simpler one may be adequate for diagnostic purposes. For the latter type of application, it may even prove beneficial to employ more than one expression to have a clearer picture of fault signatures.

VI. Conclusions

A method for the analytical representation of compressor and turbine performance maps has been presented. The effectiveness of the method has been demonstrated by application to engine test cases. The methods described in this paper have been used for modeling a variety of engines, and it is almost always possible to find a model that accurately represents a component map. In some cases, however, the required model may be quite complicated, using numerous parameters. The level of sophistication of the model will have to be chosen to offer an accurate description of the map without introducing too many parameters.

Appendix: Estimation of Model Parameters

The function to be minimized to calculate the required values of the model parameters is

$$\chi^2 = \sum_{i=1}^{\mathrm{NP}} \left[\frac{Y_G - F(X_G; a)}{\sigma_i^2} \right]^2 \tag{A1}$$

where X_G and Y_G are the NP known values of the engine performance parameters. In the case of a linear model, and ignoring the standard deviation of the measurements that is usually unknown, the maximum likelihood estimator for α is derived from the following relations:

$$\frac{\partial \chi^2}{\partial \alpha_i} = 0, \qquad i = 1, N \Rightarrow \sum_{i=1}^{\mathrm{NP}} \left[y_i - \sum_{j=1}^{N} \alpha_j \cdot F_j(X, \bar{n}) \right]$$

$$\times F_k(X, \bar{n}) = 0, \quad k = 1, N \tag{A2}$$

and if we define

$$A\colon A_{ij} = F_j(X_i, \bar{n}_i)$$
$$\boldsymbol{b}\colon b_i = y_i \tag{A3}$$

the previous expression becomes

$$(A^T \cdot A) \cdot a = A^T \cdot \boldsymbol{b} \tag{A4}$$

which is the system of normal equations for the least-squares problem. Instead of solving this problem directly, we rewrite Eq. (A4) in the following form:

$$\chi^2 = |A \cdot a - \boldsymbol{b}|^2 \rightarrow \text{minimum } (A\colon \mathrm{NP} \times N) \tag{A5}$$

Using singular value decomposition, we can write A as

$$A = U \cdot W \cdot V^T \tag{A6}$$

where U is a NP $\times$ N column orthogonal matrix, W is an $N \times N$ diagonal matrix with nonnegative elements, and V is a $N \times N$ orthogonal matrix. In that case, α will be

$$a = V \cdot \tilde{W} \cdot U^T \cdot \boldsymbol{b}$$

where

$$\tilde{W}\text{: } \tilde{w}_{ij} = 1/w_{ij} \tag{A7}$$

The advantage of the method is that singular values that appear in the form $w_{ij} = 0$ can be neglected, setting $1/w_{ij} = 0$. In addition to that, even nonsingular but very small w_{ij} values can be left out of the computation, as they increase the probable error in the estimation of the model parameters.

In the case of nonlinear models, we use a variation of the Levenberg–Marquadt method.[12] This method is based on expressing the χ^2 function through a Taylor-series expansion as

$$\chi^2 = \chi^2(a_0) + \sum_i \frac{\partial \chi^2}{\partial \alpha_i} + \frac{1}{2} \sum_{i,j} \frac{\partial^2 \chi^2}{\partial \alpha_i \partial \alpha_j} + \cdots$$

$$= \gamma - d \cdot a + \frac{1}{2} a \cdot D \cdot a \tag{A8}$$

where

$$\gamma \equiv \chi^2(a_0), \qquad d \equiv -\nabla \chi^2 \big|_{a_0}, \qquad D_{ij} = \frac{\partial^2 \chi^2}{\partial \alpha_i \partial \alpha_j}\bigg|_{\alpha_0}$$

It is now easy to calculate the function's gradient as

$$\nabla \chi^2 = D \cdot a - \boldsymbol{d} \tag{A9}$$

In case the form of x^2 is quadratic, the minimum is directly obtainable from the solution of $D \cdot \delta\alpha - d = 0$. If it is not, we can use the steepest descent method to move to a new location setting

$$a_{\text{new}} = a_{\text{old}} - c \times \nabla \chi^2(a_0) \tag{A10}$$

where c is small enough not to exhaust the downhill direction.

The quantities needed for the calculation are the first and second derivatives of χ^2, with respect to the model parameters. They are easily derived and are equal to

$$-2 \cdot b_j = \frac{\partial \chi^2}{\partial \alpha_j} = -2 \sum_{i=1}^{\text{NP}} \left[y_i - F(X_i, \bar{n}_i; a) \cdot \frac{\partial F(X_i, \bar{n}_i; a)}{\partial \alpha_j} \right]$$

$$j = 1, N \tag{A11}$$

$$2 \cdot A_{jl} = \frac{\partial^2 \chi^2}{\partial \alpha_j \partial \alpha_l} = 2 \cdot \sum_{i=1}^{\text{NP}} \left[\frac{\partial F(X_i, \bar{n}_i; a)}{\partial \alpha_j} \cdot \frac{\partial F(X_i, \bar{n}_i; a)}{\partial \alpha_l} \right]$$

$$- 2 \cdot \sum_{i=1}^{\text{NP}} \left\{ [y_i - F(X_i, \bar{n}; a)] \cdot \frac{\partial^2 F(X_i, \bar{n}; a)}{\partial \alpha_l \partial \alpha_j} \right\} \tag{A12}$$

The term involving the second derivative can be destabilizing, and as it is multiplied by $(y_i - F_i)$, which should be close to zero for a good model, it is not included. With the previous definitions for A and b, we can write Eqs. (A9) and (A10) in the form

$$\begin{aligned} A \cdot \delta a &= \boldsymbol{b} \quad \text{(quadratic)} \\ \delta a &= c \times \boldsymbol{b} \quad \text{(steepest descent)} \end{aligned} \tag{A13}$$

If we introduce the matrix A', such that

$$A'_{ij} = A_{ij}, \qquad A'_{ii} = (1 + \lambda) \cdot A_{ii} \tag{A14}$$

Using A' instead of A in Eq. (A13), we can switch between the two methods (steepest descent and direct calculation with a quadratic form), because the equation becomes diagonally dominant and reduces to $\delta\alpha_i = 1/(\lambda \cdot A_{ii}) \cdot b_i$ for large values of λ. It is thus possible to switch between the two methods, increasing λ when χ^2 increases and decreasing it when χ^2 decreases.

To evaluate the error involved in the estimation of the model parameters, we will need to determine the covariance matrices for these parameters.

In case a singular value decomposition method is used, the covariance matrix for the model parameters can be proven to be

$$Y_{jk} = \sum_{i=1}^{N} \left(\frac{V_{ji} V_{ki}}{w_i^2} \right) \tag{A15}$$

whereas for nonlinear methods we have $Y = A$.

It is now possible to determine the confidence region for each of the parameters at a specified level p (e.g., $p = 95\%$), as

$$\alpha_j \pm t \left(Np - N, \frac{1 + p}{2} \right) \cdot \sigma(\alpha_j), \qquad \sigma(\alpha_j) = \sqrt{Y_{jj}} \tag{A16}$$

where t is the variable of Student's distribution with NP $-$ N degrees of freedom. A more general expression is the confidence ellipsoid, given by

$$(\boldsymbol{a} - a)^T \cdot Y^{-1} \cdot (\boldsymbol{a} - a) \leq F(N, \text{NP} - N, p) \tag{A17}$$

where F is the F-distribution variable at a confidence level p, and a is the estimated array of parameters.

This expression allows us to examine a whole set of parameters to determine whether it is significantly different from a previous one.

It should be noted that the confidence regions mentioned earlier are not entirely reliable because they do not include the influence of the measurements' deviation, but they are a good indicator as to whether a change is significant.

References

[1]Bird, J. W., and Schwarz, H. M., "Diagnosis of Turbine Engine Transient Performance with Model Based Parameter Estimation Techniques," American Society of Mechanical Engineers, Paper 94-GT-317, June 1994.

[2]El-Gammal, A. M., "An Algorithm and Criteria for Compressor Characteristics Real Time Modelling and Approximation," American Society of Mechanical Engineers, Paper 90-GT-336, June 1990.

[3]Flack, R. D., "Analysis and Matching of Gas Turbine Components," *International Journal of Turbo and Jet Engines*, Vol. 7, 1990, pp. 217–226.

[4]French, M. W., "Development of a Compact Real-Time Turbofan Engine Dynamic Simulation," Society of Automotive Engineers, Paper 821401, Oct. 1982.

[5]Horlock, J. H., *Axial Flow Compressors*, Krieger, Malabar, FL, 1973.

[6]Mattingly, J. D., *Elements of Gas Turbine Propulsion*, McGraw–

Hill, New York, ISBN 0-07-114521-4, 1996.

[7]Vinnemeier, F., and Koschel, W., "Strömungsmessungen in mehrstufigen Axialverdichter, VDI Berichte NR.706, 1988.

[8]Wenzel, L. M., Moss, J. E., and Mehalic, C. M., "Effect of Casing Treatment on the Performance of a Multistage Compressor," NASA TMx-3175, Jan. 1975.

[9]Carchedi, F., Campling, A. M., Hannis, J. M., and Wood, G. R., "Design and Development of the Ruston Typhoon Gas Turbine," *Turbomachinery International*, May/June 1989, pp. 31–37.

[10]Horlock, J. H., *Axial Flow Turbines*, Krieger, Malabar, FL, 1973.

[11]Stamatis, A., Mathioudakis, K., and Papailiou, K. D., "Adaptive Simulation of Gas Turbine Performance," *Journal of Engineering for Gas Turbines and Power*, Vol. 112, 1990, pp. 168–175; also American Society of Mechanical Engineers, Paper 89-GT-205, June 1989.

[12]Press, W. H., Flannery, B. P., Teukolsky, S. A., and Vetterling, W. T., *Numerical Recipes*, Cambridge Univ. Press, Cambridge, England, UK.